Journal Pre-proofs

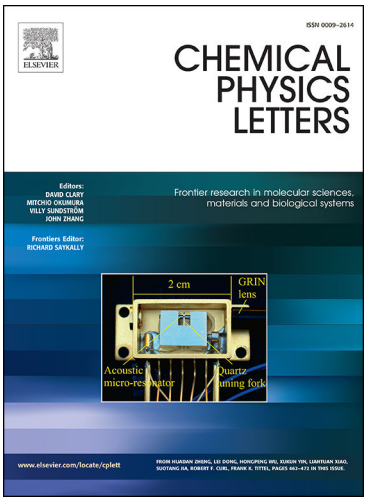

Research paper

Benchmark calculations of the ^1D Rydberg spectrum of beryllium.

Monika Stanke, Ewa Palikot, Keeper L. Sharkey, Ludwik Adamowicz

PII: S0009-2614(21)00506-6
DOI: https://doi.org/10.1016/j.cplett.2021.138823
Reference: CPLETT 138823

To appear in: *Chemical Physics Letters*

Received Date: 27 April 2021
Revised Date: 8 June 2021
Accepted Date: 9 June 2021

Please cite this article as: M. Stanke, E. Palikot, K.L. Sharkey, L. Adamowicz, Benchmark calculations of the ^1D Rydberg spectrum of beryllium., *Chemical Physics Letters* (2021), doi: https://doi.org/10.1016/j.cplett.2021.138823

Monika Stanke*
Institute of Physics, Faculty of Physics, Astronomy, and Informatics,
Nicolaus Copernicus University, ul. Grudziądzka 5, Toruń, PL 87-100, Poland*

Ewa Palikot and Keeper L. Sharkey
Department of Chemistry and Biochemistry, University of Arizona, Tucson, Arizona 85721, USA†

Ludwik Adamowicz‡
Department of Chemistry and Biochemistry and Department of Physics,
University of Arizona, Tucson, Arizona 85721, USA and
Interdisciplinary Center for Modern Technologies,
Nicolaus Copernicus University, ul. Wileńska 4, Toruń, PL 87-100, Poland

ABSTRACT

High-accuracy calculations are performed on the ^1D spectrum of beryllium with the use of all-electron explicitly correlated Gaussian (ECG) functions. In the first step, a nonrelativistic wave function is generated for each state with the ECG nonlinear parameters variationally optimized using a procedure employing energy gradient determined with respect to these parameters. The wave functions are used to calculate the leading relativistic corrections employing the recently implemented algorithms. The state total energies and the interstate transition energies are compared with the high-quality experimental results.

I. INTRODUCTION

The ultimate criterion for refining theoretical methods for calculating atomic electronic structures and spectra is the comparison with high-precision experimental measurements. Precision spectroscopy of the light elements has been quickly advancing in recent years resulting in the need for refining the methods for high-accuracy quantum-mechanical atomic calculations. Model systems frequently used for verifying the theoretical atomic-calculation models are the beryllium atom and beryllium-type ions. For these systems, the presently available computational resources are, in general, sufficient to achieve adequate convergence of the calculations in terms of the basis set size. Thus, the remaining cause of the uncertainties is mainly limited to the theoretical model used to describe the interactions and other effects present in the atom. The trend in improving the theoretical model is very well demonstrated in recent calculations

*Electronic address: monika@fizyka.umk.pl
†Electronic address: epalikot@gmail.com
‡Electronic address: ludwik@email.arizona.edu

and with the account of the leading relativistic and quantum electrodynamics (QED) corrections [1–4]. The nonrelativistic ground-state energy of beryllium was also recently calculated using the Hylleraas-configuration-interaction (Hy-CI) method [5]. One should also mention the recent Hy-CI calculations of a large number of energy levels for both singlet and triplet excited states of beryllium performed with the millihartree precision [6, 7] and high-accuracy ECG isotope-shift calculations of some lowest beryllium Rydberg states performed with the inclusion of the leading relativistic and QED corrections [8].

The beryllium Rydberg ^1D spectrum was a subject of nonrelativistic calculations carried out by our group [9]. However, as those calculations did not include the relativistic corrections, the results were off from the experimental values by more than the uncertainties of the experimental results. This deficiency is eliminated in the present work due to the inclusion of the leading relativistic corrections. However, the present calculations still do not include the leading QED corrections that usually contribute approximately a tenth of a wavenumber to the interstate transition energies.

The beryllium energy levels and the corresponding interstate transitions energies have been a subject of several precision measurements performed over the last half century. In particular, one should mention the 1953 work of Bozman et al. [10] and Johansson [11]. The latter author measured an array of transitions with 0.01-0.02 cm^{-1} precision. Johansson measurements also included a transition involving the lowest D state, i.e. the $2s2p\ ^1P \rightarrow 2s3d\ ^1D$ transition. The absolute energy of the lowest ^1D state beryllium was also first measured by Johansson to be 64 428.31(10) cm^{-1} [12]. The precision of the measurement of this quantity was recently increased 180 fold by Cook et al. [13] who obtained the value of 64 428.40 321(55) cm^{-1} for this quantity.

Accurate description of the electron correlation effects is key in precision calculations of atomic spectra. These effects originate from electrostatic repulsion of the electrons and a decrease of the probability of finding two or more electrons close to each other. The most effective approach to represent this probability decrease in the wave function is making the basis functions used to expand the spatial part of the wave function explicitly dependent on the inter-electron distances. ECGs are such functions. However, as the ECGs depend exponentially on the squares of the internuclear distances, they do not strictly satisfy the Kato cusp conditions. This deficiency can be effectively remediated by increasing the size of the ECG basis set and by performing a thorough variational optimization of the ECG exponential parameters [14–17]. This is how the calculations described in this work are performed.

The use of the all-electron ECGs in atomic calculations is convenient because the formulas for the Hamiltonian and overlap matrix elements for these functions are relatively simple and can be coded into a computer program in a general form for an arbitrary number of electrons in the system. Also, ECGs for expanding the wave functions corresponding to atomic states with different non-zero angular momentum quantum numbers, L, can be easily constructed by multiplying the S-type ECGs by appropriate Cartesian spherical harmonics. In this way, the basis functions for expanding wave functions of atomic D states were constructed in our previous works [20, 21].

The high accuracy of the atomic ECG calculations is exemplified by, for example, our previous works on lowest S and P Rydberg states of four- and five-electron atoms [14–17]. It should also be mentioned, that, even though

and nitrogen atoms [18, 19], the use of these codes to accurately calculate the spectra of these systems require an allotment computer time which is currently out of reach to our group.

The optimization of the ECG exponential parameters is the most time-consuming part of our atomic calculations especially when the size of the basis set becomes large. To expediate the optimization, we developed procedures for calculating the analytical energy gradient determined with respect to these parameters [14–17]. The formulas for calculating the gradient matrix elements are slightly more complicated than those used to calculate the Hamiltonian and overlap matrix elements, but they have closed forms and can be calculated almost as fast as the latter matrix elements. The formulas for the energy-gradient matrix elements for atomic D states were derived an implemented in our previous work [20]. The work also included the formulas for the Hamiltonian and overlap matrix elements. When the energy gradient is provided to the procedure that runs the parameter optimization, the variational lowering of the energy advances much faster than without the gradient. The situation is similar to the optimization of a molecular structure in a calculation where the wave function of the system is expanded in terms of orbital Gaussians. There also, when the analytical gradient of the total energy of the system determined with respect to the geometrical parameters of the structure of the molecule is provided to the procedure that runs the search for the equilibrium molecular geometry, the determination of this geometry proceeds much faster than if the gradient is not available. The gradient aided optimization of the exponential parameters of the ECGs is key in achieving high accuracy in the calculations.

The internal motion of the particles forming the atom involves a coupled motion of the electrons and the nucleus around the center of mass of the system. Bound quantum states representing this motion in the beryllium atom and corresponding to $L = 2$ and $M_L = 0$ are the states considered in the present work. Unlike in the conventional approach, where that the nuclear mass is usually assumed to be infinite and the nuclear motion is excluded from the consideration (the effects related to this motion can subsequently be included as corrections obtained using the perturbation-theory calculations), in the present approach, the finite nuclear mass is present in the model starting from the first step of the calculations. This first step is the variational calculation of the nonrelativistic energy and the corresponding wave function of each considered state of the system. In this calculation, the ECG basis set for that state is generated and optimized. The inclusion of the finite mass of the nucleus in the model is done using a Hamiltonian, called the internal Hamiltonian, that explicitly depends on the nuclear mass. The Hamiltonian is obtained by subtraction out the operator representing the kinetic energy of the motion of the center-of-mass of the atom from the laboratory-frame non-relativistic Hamiltonian of the system. This Hamiltonian consists of the kinetic energy operators representing the motions of the nucleus and the electrons and the operators representing all electrostatic interactions present in the atom. If, before the subtraction, the lab-frame nonrelativistic Hamiltonian is transformed from the lab-frame Cartesian coordinate system to a new system of coordinates whose first three coordinates are the lab-frame coordinates of the center-of-mass and the remaining coordinates are the so-called internal coordinates, the Hamiltonian automatically and rigorously separates into the operator representing the kinetic energy of the center-of-mass motion and the internal Hamiltonian (see the next section). The energies and the wave functions calculated with

used to calculate the interstate nonrelativistic transition energies of the isotope and the isotope shifts of these energies. In the case of the beryllium atom which has only one stable isotope, ^{9}Be, the shifts calculated in this work are the differences between the corresponding transition energies of ^{9}Be and $^\infty$Be.

The present calculations include the leading relativistic corrections. The algorithms for calculating these corrections were recently implemented [21]. The operators representing the corrections are obtained by transforming the lab-frame relativistic operators to the internal coordinates. The transformed operators are used to calculate the corrections as expectation values with the wave functions obtained from the finite-nuclear-mass nonrelativistic calculations. Thus, the corrections explicitly include the so-called recoil effects, i.e., the relativistic effects associated with the motion of the nucleus about the center of mass.

II. THE METHOD

A. The Hamiltonian

The center of the internal coordinate system used in this work is placed at the nucleus of the atom and the internal coordinates are the Cartesian coordinates of the vectors, $\mathbf{r}_i$, $i = 1, \ldots, n$ (n is the number of the electrons in the atom) that have their origins in the center of the coordinate system and the ends at the different electrons. The internal Hamiltonian has the following form:

$$\hat{\mathrm{H}} = -\frac{1}{2}\left(\sum_{i=1}^{n}\frac{1}{\mu_i}\nabla_{\mathbf{r}_i}^T\cdot\nabla_{\mathbf{r}_i} + \frac{1}{m_0}\sum_{\substack{i,j=1\\ i\neq j}}^{n}\nabla_{\mathbf{r}_i}^T\cdot\nabla_{\mathbf{r}_j}\right) + \sum_{i=1}^{n}\frac{q_0 q_i}{r_i} + \sum_{i>j=1}^{n}\frac{q_i q_j}{r_{ij}}, \tag{1}$$

where m_0 is the mass of the nucleus and q_0 is its charge, q_i are electron charges, and $\mu_i = m_0 m_i/(m_0 + m_i)$ are electron reduced masses (m_i, $i = 1, \ldots, n$, are the electron masses). T in (1) denotes the matrix/vector transpose (this notation is used throughout this work). The internal Hamiltonian, Eq. (1), represents the motion of n particles, whose charges are the electron charges and the masses are the reduced electron masses, in the central field of the charge of the nucleus. We call these particles the "pseudo-electrons". As one notices, the approach used in the derivation of the internal Hamiltonian is the same as the standard textbook approach used for the hydrogen atom.

The motions for the pseudo-electrons in (1) are coupled through the Coulombic interactions, $\sum_{i=1}^{n}\frac{q_0 q_i}{r_i} + \sum_{i>j=1}^{n}\frac{q_i q_j}{r_{ij}}$, where $r_{ij} = |\mathbf{r}_j - \mathbf{r}_i|$, and through the so-called mass-polarization term, $-\frac{1}{2}\sum_{\substack{i,j=1\\ i\neq j}}^{n}(1/m_0)\,\nabla_{\mathbf{r}_i}^T\cdot\nabla_{\mathbf{r}_j}$. Hamiltonian (1) is used to grow and optimize the basis set and to calculate the nonrelativistic energy and the corresponding wave function for each state considered in the present work.

The special part of the wave function for a D state of the beryllium atom considered in the present work is expanded in terms of the basis functions being the following products of Gaussian exponentials and Cartesian angular harmonics:

$$\phi_k^{(L=2)} = \left(x_{i_k}x_{j_k} + y_{j_k}y_{i_k} - 2z_{i_k}z_{j_k}\right)\exp\left[-\mathbf{r}^T\left(A_k \otimes I_3\right)\mathbf{r}\right], \tag{2}$$

where electron labels i_k and j_k can vary from 1 to n, with $i_k \geq j_k$. i_k and j_k can either be equal or not equal to each other. For the beryllium atom $n = 4$. A_k in (2) is an $n \times n$ symmetric matrix of the exponential parameters. This matrix is unique to each ECG. $\otimes$ denotes the Kronecker product, I_3 is an 3×3 identity matrix, and $\mathbf{r}$ is the following $3n$ vector of the internal Cartesian coordinates:

$$\mathbf{r} = \begin{pmatrix} \mathbf{r}_1 \\ \mathbf{r}_2 \\ \vdots \\ \mathbf{r}_n \end{pmatrix} = \begin{pmatrix} x_1 \\ y_1 \\ z_1 \\ \vdots \\ x_n \\ y_n \\ z_n \end{pmatrix}. \tag{3}$$

We denote $(A_k \otimes I_3)$ in (2) as $\mathbf{A}_k$.

As the considered states are bound states, the basis functions (2) need to be square integrable. In order for this to happen $\mathbf{A}_k$ has to be positive definite. To achieve this, $\mathbf{A}_k$ is represented in the following Cholesky-factored form: $\mathbf{A}_k = (L_k L_k^T) \otimes I_3$, where L_k is a $n \times n$ lower triangular matrix. If all matrix elements of L_k are real numbers, $\mathbf{A}_k$ becomes automatically positive definite. The matrix elements of L_k are the variational parameters in the calculations performed in this work. As these parameters can be varied without any restrictions in the range from $-\infty$ to $+\infty$, the optimization of these parameters is unconstrained. This is always a desirable feature in any multiparameter optimization.

We use the so-called spin-free formalism to impose the proper permutational symmetry of the wave function in the present calculations [22–24]. The formalism involves the construction of an appropriate symmetry projector, P, that by acting on the special part of each basis function implements the desired permutational symmetry. P is constructed using the standard procedure that employs the appropriate Young operator specific to the spin state of the system [22–24]. The construction of the Young operators in the ECG calculations was described in our earlier work [25]. For ^1D states of the beryllium atom, the symmetry projector can be chosen as: $P = (1 - P_{13})(1 - P_{24})(1 + P_{12})(1 + P_{34})$, where P_{ij} permutes the spatial coordinates of the i-th and j-th electrons.

The internal Hamiltonian and the operators representing the relativistic corrections are symmetric with respect to any permutation of the electron labels. Thus, in calculating the corresponding matrix elements (integrals), the symmetry operator can be placed only in the "ket" part of the integral. It appears there as $P^\dagger P$. For beryllium, $P^\dagger P$ consists of $4! = 24$ terms. Thus, each matrix element is a sum of 24 different elementary spatial integrals. The

...tical energy gradient vector with ECGs (2), were presented in Ref. [20].

C. Relativistic operators

The leading relativistic correction of the order of α^2, where α is the fine-structure constant ($\alpha = \frac{1}{c}$, where c is the speed of light in the atomic units), includes the mass-velocity (MV), Darwin (D), orbit-orbit (OO), and spin-spin (SS) effects. As the considered states are singlet states, the spin-orbit interaction vanishes. In the internal coordinate system, the MV, D, OO, and SS operators have the following forms:

mass-velocity term:

$$\hat{H}_{\mathrm{MV}} = -\frac{1}{8}\left[\frac{1}{m_0^3}\left(\sum_{i=1}^{n}\nabla_{\mathbf{r}_i}\right)^4 + \sum_{i=1}^{n}\frac{1}{m_i^3}\,\nabla_{\mathbf{r}_i}^4\right], \tag{4}$$

Darwin term:

$$\hat{H}_{\mathrm{D}} = \frac{\pi}{2}\sum_{i=1}^{n}\left(\frac{4}{3}\frac{1}{m_0^2} + \frac{1}{m_i^2}\right) q_0 q_i\,\delta^3(\mathbf{r}_i) + \frac{\pi}{2}\sum_{i=1}^{n}\sum_{j\neq i}^{n}\frac{1}{m_i^n}\,q_i q_j\,\delta^3(\mathbf{r}_{ij}), \tag{5}$$

orbit-orbit term:

$$\begin{aligned}\hat{H}_{\mathrm{OO}} \;=\; & -\frac{1}{2}\sum_{i=1}^{n}\sum_{j=1}^{n}\frac{q_0 q_j}{m_0 m_j}\left[\frac{1}{r_j}\nabla_{\mathbf{r}_i}{}^T\cdot\nabla_{\mathbf{r}_j} + \frac{1}{r_j^3}\,\mathbf{r}_j^T\cdot(\mathbf{r}_j^T\cdot\nabla_{\mathbf{r}_i})\nabla_{\mathbf{r}_j}\right] \\ & +\frac{1}{2}\sum_{i=1}^{n}\sum_{j>i}^{n}\frac{q_i q_j}{m_i m_j}\left[\frac{1}{r_{ij}}\nabla_{\mathbf{r}_i}^T\cdot\nabla_{\mathbf{r}_j} + \frac{1}{r_{ij}^3}\,\mathbf{r}_{ij}^T\cdot(\mathbf{r}_{ij}^T\cdot\nabla_{\mathbf{r}_i})\nabla_{\mathbf{r}_j}\right],\end{aligned} \tag{6}$$

and spin-spin term:

$$H_{\mathrm{SS}} = -\frac{8\pi}{3}\sum_{\substack{i,j=1\\ j>i}}^{4}\frac{q_i q_j}{m_i m_j}\left(\mathbf{s}_i\cdot\mathbf{s}_j\right)\delta\left(\mathbf{r}_{ij}\right), \tag{7}$$

where $\delta(\mathbf{r})$ is the Dirac delta function, $\nabla_{\mathbf{r}_i}$ is the usual nabla operator acting on the coordinates of vector $\mathbf{r}_i$, and $\mathbf{s}_i$ is the spin operator for electron i. For the states considered in this work $\mathbf{s}_i\cdot\mathbf{s}_j = -3/4$. The formulas for the matrix elements of the above relativistic operators were presented in our recent paper [21].

D. The calculations

The present calculations are performed using double precision. In the first step of the calculations, the nonrelativistic energies and the corresponding wave functions are determined for the lowest nine ^1D states of beryllium. For each state, the basis set is generated in a separate calculation that involves growing the set from a small number of functions to the final basis set of 13500 ECGs using a procedure consisting of adding a certain number of functions one by one and optimizing them. The optimization involves the use of the analytical energy gradient. After a certain number of functions is added to the basis set (usually 100 functions), the whole set is reoptimized using one-function-at-a-time

addition of a basis function or after an optimization of a basis function, the overlap integrals of the function with all other functions in the basis set are checked and, if any of them exceeds an assumed threshold (e.g. 0.99), the function is removed from the set and a new function is added in its place and optimized. A linear dependency among the basis functions is undesirable because it may cause numerical instabilities in the calculation. The standard procedure is used to solve the secular equation problem and to determine the linear expansion coefficients, c_k, of the wave function in terms of the ECGs and the corresponding total nonrelativistic energy. The basis set optimizations are carried out for the ^{9}Be isotope. After the basis-size reaches the size of 13500 functions for a particular state, the basis set is used to determine the energy and the corresponding wave function for that state for $^{\infty}$Be without reoptimization of the Gaussian exponential parameters. As our previous calculations of S, P, and D states of atomic isotopomers showed [20], a reoptimization of the nonlinear variational parameters is not needed when states of different isotopologues are calculated. A recalculation of the c_k expansion coefficients usually suffices to account for small changes of the total energy and the wave function caused by the change of the nuclear mass [21]. The process of growing the basis sets for the nine ^{1}D states is by far the most time-consuming part of the calculations. These calculates have lasted for several months. More details concerning the procedure used in growing the ECG basis set and in optimizing the Gaussian exponential parameters are described in our previous paper [21].

The nonrelativistic wave functions obtained for the nine lowest states of ^{9}Be and $^{\infty}$Be are used in the calculations of the relativistic corrections. After adding these corrections to the nonrelativistic energies, the interstate transition energies are calculated.

III. RESULTS

The calculations are performed using a computer code written in Fortran 90 that employs the MPI (message passing interface) protocol for parallelization. The procedures for calculating the MV, D, OO, and SS relativistic corrections were recently added to the code [21]. The present work is the first full-scale application of the code to perform high-accuracy study of a spectrum of Rydberg D states of a four-electron atom.

The first set of results concerns the nonrelativistic calculations. The results are shown in Table I. For each state the results include the total ^{9}Be nonrelativistic energies obtained with 10800, 11700, 12600, 13500, and 14400 ECGs and the $^{\infty}$Be energies obtained with 14400 ECGs. The ^{9}Be results allow for assessing the convergence of the nonrelativistic energies in terms of the number of Gaussians in the basis set. As one can see, for the first five states, the increase of the basis set size by almost a thousand results in the decrease of the energy value expressed in hartrees in the ninth digit after the decimal point. For the sixth state, the corresponding energy decrease is about 2×10^{-8}, for the seventh state, it is 5×10^{-8}, and for the ninth state, it is 2×10^{-7}. This type of the convergence pattern is expected. As the excitation level increases, the number of the radial nodes in the wave function also increases and this leads to the need to increase the number of ECGs in the basis set. When the same number of basis functions is used for all considered states, the lower states are represented somewhat better than the upper states. The results suggest that the basis set for the seventh, eighth, and ninth states should be, perhaps, grown more so that a similar convergence level of the

The convergence of the one- and two-electron Dirac delta functions, δ_{r_i} and $\delta_{r_{ij}}$, the mass-velocity, Darwin, orbit-orbit, and spin-spin relativistic corrections, and the total relativistic correction, ΔE_r, for each of the nine considered states of ^{9}Be are shown in Table II. The calculations of these quantities are performed for ^{9}Be for basis sets of 5100, 6000, and 6900 ECGs (5100, 6200, and 7100 for state 4^1D).

The corrections obtained with 6900 ECGs are added to the nonrelativistic energy obtained with the 13500 ECGs to obtain the most accurate total energy that this work provides for each considered state. However, in order for this procedure to work, the total relativistic correction needs to be well convergent at the 6900 ECG level. The ΔE_r value show in Table II. It should be noted that the relativistic correction shown in the last column of the table is multiplied by α^2 before it is added to the nonrelativistic energy to generate the final energy of each ^1D state of ^{9}Be. Upon examining the values of ΔE_r one notices that for the lowest six states the results in going from 6000 to 6900 ECGs change in the eighth figure after the decimal point. For the last three states the change is the seventh figure. This convergence level is sufficient to produce the interstate transition energies with accuracy similar or better than the accuracy of the presently available experimental data. Table II also includes the relativistic corrections for $^\infty$Be obtained with the 6900 ECGs. The total energies that include the relativistic corrections for the lowest nine ^1D states of ^{9}Be and $^\infty$Be are shown in Table III. The results are obtained by adding the 6900-ECG relativistic corrections to the corresponding nonrelativistic energies obtained with 14400 ECGs. The difference between the relativistic corrections of ^{9}Be and $^\infty$Be accounts for the recoil effects. As one can see, this effect lowers the relativistic correction by only 0.000000065 hatree for the lowest $1s^22p^2$ state with respect to the $^\infty$Be result. The lowering is equal to 0.000000098 hartree for the $1s^22s3d$ state, and 0.000000088-0.000000090 hartree for the next seven states. As the lowering is only of the order of 0.002 cm^{-1}, it has a negligible effect on the transition energies discussed next.

The nonrelativistic ^{9}Be and $^\infty$Be energies and the energies obtained by adding the relativistic corrections to the nonrelativistic energies are used to calculate the interstate transition energies between adjacent ^1D states. A comparison between the calculated and experimental results are shown in Table IV. As one can see, for the lowest $1s^22p^2 \rightarrow 1s^22s3d$ transition, the finite mass effect contributes to the transition energy about 3 cm^{-1}. The contribution from the relativistic effects has an opposite sign and amounts to about -10 cm^{-1}. The finite-mass effects and the relativistic corrections are much smaller for transitions between higher excited states. For example, for the $1s^22s4d \rightarrow 1s^22s5d$ transition, the finite-mass correction is only about 0.05 cm^{-1} while the relativistic correction is about 0.40 cm^{-1}. For the lowest transition, our best result of 7545.745(0.020) cm^{-1} agrees with the experimental value of 7545.8558(0.0215) cm^{-1} within 0.1 cm^{-1}. For the $1s^22s4d \rightarrow 1s^22s5d$ transition, the best calculated energy is 2221.480(0.030) cm^{-1} and the experimental energy of 2221.446(0.1) cm^{-1} is only by about 0.03 cm^{-1} lower. The estimates of the uncertainties of the transition energies calculated at the ΔE_{nr} (^{9}Be) + ΔE_r (^{9}Be) level are shown in parenthesis. The estimates correspond to the uncertainties due to using incomplete basis sets in the calculations of the nonrelativistic energies and the relativistic corrections (not to neglecting higher order effects).

In summary, transition energies between the adjacent nine lowest ^1D Rydberg states (i.e. singlet $L = 2\, M_L = 0$ states) of beryllium are calculated using the finite-nuclear-mass approach and with the inclusion of the leading relativistic corrections. The algorithms for calculating these corrections were recently implemented [21]. The nonrelativistic wave functions of the considered states are expanded in terms of explicitly correlated Gaussian functions. 13500 ECGs are used for each state. The calculated transition energies agree well with the experimental values. However, the agreement can certainly be improved by including the leading quantum electrodynamics (QED) effects. Algorithms for calculating these effects will be derived and implemented in our future work.

Acknowledgments

This work of M.S has been supported by the Polish National Science Centre; grant DEC-2013/10/E/ST4/00033. It has also been supported by a grant from the National Science Foundation; grant no. 1856702. The authors are grateful to the University of Arizona Research Computing for providing computational resources for this work.

[1] M. Puchalski, J. Komasa, and K. Pachucki, Phys. Rev. A 87, 030502(R) (2013).

[2] M. Stanke, J. Komasa, S. Bubin, and L. Adamowicz, Phys. Rev. A 80, 022514 (2009).

[3] I. Hornyák, L. Adamowicz, and S. Bubin, Phys. Rev. A 100, 032504 (2019).

[4] E. C. Cook, A. D. Vira, C. Patterson, E. Livernois, and W. D. Williams, Phys. Rev. Lett. 121, 053001 (2018).

[5] J. S. Sims and S. A. Hagstrom, J. Chem. Phys. 140, 224312 (2014).

[6] M. B. Ruiz, F. Latorre, and A. M. Frolov, in Electron Correlation in Molecules ab initio Beyond Gaussian Quantum Chemistry, Advances in Quantum Chemistry, Vol. 73, edited by P. E. Hoggan and T. Ozdogan (Academic Press, Cambridge, 2016), pp. 119–138.

[7] A. M. Frolov and M. B. Ruiz, Chem. Phys. Lett. 595-596, 197 (2014).

[8] M. Puchalski, K. Pachucki, and J. Komasa, Phys. Rev. A 89, 012506 (2014).

[9] K. L. Sharkey, S. Bubin, and L. Adamowicz, Phys. Rev. A 84, 044503 (2011).

[10] W. R. Bozman, C. H. Corliss, W. F. Meggers, and R. E. Trees, J. Res. Natl. Bur. Stand. 50, 131 (1953).

[11] L. Johansson, Ark. Fys. 23, 119 (1963).

[12] A. Kramida, Yu. Ralchenko, J. Reader, and NIST ASD Team, NIST Atomic Spectra Database (Version 5.7.1), https://physics. nist.gov/asd (National Institute of Standards and Technology, Gaithersburg, 2019).

[13] E. C. Cook, A. D. Vira, and W. D. Williams, Phys. Rev. A 101, 042503 (2020).

[14] M. Stanke, D. Kędziera, S. Bubin, and L. Adamowicz, Phys. Rev. Lett. 99, 043001 (2007).

[15] S. Bubin, J. Komasa, M. Stanke, and L. Adamowicz, Phys. Rev. A 81, 052504 (2010).

[16] S. Bubin, J. Komasa, M. Stanke, and L. Adamowicz, J. Chem. Phys. 132, 114109 (2010).

[17] S. Bubin, M. Stanke, and L. Adamowicz, J. Chem. Phys. 131, 044128 (2009).

[18] K. L. Sharkey, M. Pavanello, S. Bubin, and L. Adamowicz, Phys. Rev. A 80, 062510 (2009).

[19] K. L. Sharkey and L. Adamowicz, J. Chem. Phys. 140, 174112 (2014).

[20] K. L. Sharkey, S. Bubin, and L. Adamowicz, J. Chem. Phys. 134, 044120 (2011).

[21] M. Stanke and L. Adamowicz, Phys. Rev. A 100, 042503 (2019).

[22] F. A. Matsen and R. Pauncz, The Unitary Group in Quantum Chemistry, Elsevier, 1986, Amsterdam.

[23] R. Pauncz, Spin Eigenfunctions, Plenum, 1979,

[24] M. Hamermesh, Group Theory and Its Application to Physical Problems, Addison-Wesley, 1962, Reading, MA.

[25] S. Bubin, M. Cafiero, and L. Adamowicz, Adv. Chem. Phys. 131, 377 (2005).

with 14400 ECGs are also shown. $1s^2$, which is common to all configurations, is omitted from the configuration designation of the state (e.g. configuration $1s^2 2p^2$ is abbreviated as $2p^2$). All values are given in a.u.

	E_{nr} (^{9}Be)					E_{nr} ($^\infty$Be)
State	10800	11700	12600	13500	14400	14400
$2p^2$	-14.407351369	-14.407351372	-14.407351374	-14.407351376	-14.407351377	-14.408237286
$2s3d$	-14.372924943	-14.372924946	-14.372924949	-14.372924950	-14.372924952	-14.373824606
$2s4d$	-14.353081965	-14.353081970	-14.353081974	-14.353081977	-14.353081979	-14.353982921
$2s5d$	-14.342957421	-14.342957427	-14.342957432	-14.342957435	-14.342957439	-14.343858137
$2s6d$	-14.337266124	-14.337266134	-14.337266141	-14.337266147	-14.337266153	-14.338166595
$2s7d$	-14.333774957	-14.333774983	-14.333775003	-14.333775019	-14.333775032	-14.334675292
$2s8d$	-14.331485295	-14.331485382	-14.331485447	-14.331485500	-14.331485551	-14.332385684
$2s9d$	-14.329903838	-14.329904083	-14.329904280	-14.329904437	-14.329904590	-14.330804633
$2s10d$	-14.328764726	-14.328765432	-14.328765988	-14.328766421	-14.328766823	-14.329666799

TABLE II. Convergence of the one- and two-electron Dirac delta functions, δ_{r_i} and $\delta_{r_{ij}}$, the mass-velocity (MV), Darwin (D), orbit-orbit (OO), and spin-spin (SS) relativistic corrections, and the total relativistic correction ΔE_r of the nine lowest ^{1}D states of ^{9}Be. The results for $^\infty$Be are also shown. $1s^2$, which is common to all configurations, is omitted from the configuration designation of the state (e.g. configuration $1s^2 2p^2$ is abbreviated as $2p^2$). The MV, D, OO, and SS corrections do not include the α^2 factor. All values are given in a.u.

State	System	Basis	δ_{r_i}	$\delta_{r_{ij}}$	MV	D	OO	SS	ΔE_r
$2p^2$	^{9}Be	4200	8.633558	0.254970	-263.578907	212.164659	-0.716925	9.612133	-0.002264196
		5100	8.633933	0.254964	-263.586368	212.174202	-0.716926	9.611901	-0.002264098
		6000	8.634379	0.254962	-263.597258	212.185448	-0.716926	9.611840	-0.002264082
		6900	8.634567	0.254950	-263.602407	212.190392	-0.716926	9.611398	-0.002264117
	$^\infty$Be	6900	8.636206	0.254995	-263.668958	212.230732	-0.691180	9.613075	-0.002264052
$2s3d$	^{9}Be	4200	8.735234	0.261564	-266.959430	214.605886	-0.878108	9.860744	-0.002309560
		5100	8.735753	0.261556	-266.974376	214.619073	-0.878108	9.860427	-0.002309670
		6200	8.736245	0.261540	-266.985919	214.631753	-0.878108	9.859827	-0.002309642
		7100	8.736281	0.261535	-266.985932	214.632738	-0.878108	9.859652	-0.002309599
	$^\infty$Be	7100	8.737868	0.261578	-267.051028	214.671813	-0.851836	9.861245	-0.002309501
$2s4d$	^{9}Be	4200	8.761854	0.263001	-267.842749	215.250677	-0.920043	9.914906	-0.002321610
		5100	8.761996	0.262958	-267.845767	215.255061	-0.920042	9.913287	-0.002321624
		6000	8.762524	0.262933	-267.859370	215.268802	-0.920042	9.912335	-0.002321667
		6900	8.762601	0.262927	-267.861287	215.270829	-0.920042	9.912130	-0.002321672
	$^\infty$Be	6900	8.764210	0.262971	-267.927220	215.310458	-0.893685	9.913767	-0.002321582
$2s5d$	^{9}Be	4200	8.767886	0.263333	-268.046505	215.396729	-0.929524	9.927435	-0.002324521
		5100	8.767945	0.263288	-268.047324	215.399082	-0.929523	9.925710	-0.002324531
		6000	8.768260	0.263240	-268.054719	215.407897	-0.929523	9.923919	-0.002324551
		6900	8.768653	0.263239	-268.061844	215.417799	-0.929523	9.923873	-0.002324405
	$^\infty$Be	6900	8.770267	0.263283	-268.127948	215.457539	-0.903145	9.925518	-0.002324317
$2s6d$	^{9}Be	4200	8.769512	0.263423	-268.106365	215.436164	-0.932789	9.930817	-0.002325602
		5100	8.769832	0.263407	-268.114479	215.444514	-0.932790	9.930211	-0.002325622
		6000	8.770364	0.263378	-268.128185	215.458433	-0.932790	9.929131	-0.002325668
		6900	8.770556	0.263365	-268.130397	215.463497	-0.932789	9.928630	-0.002325543
	$^\infty$Be	6900	8.772171	0.263409	-268.196555	215.503274	-0.906403	9.930278	-0.002325455

State	System	Basis	o_{r_i}	$o_{r_{ij}}$	MV	D	OO	SS	ΔE_r
		4200	8.768005	0.263574	-268.085616	215.395531	-0.934227	9.936522	-0.002326434
		5100	8.770340	0.263460	-268.152689	215.456394	-0.934227	9.932209	-0.002326994
$2s7d$	^{9}Be	6000	8.770562	0.263432	-268.156083	215.462514	-0.934228	9.931145	-0.002326906
		6900	8.770928	0.263420	-268.154863	215.471938	-0.934229	9.930686	-0.002326364
	$^{\infty}$Be	6900	8.772544	0.263463	-268.221043	215.511729	-0.907838	9.932335	-0.002326276
		4200	8.765105	0.263781	-268.035300	215.318809	-0.934968	9.944314	-0.002327465
		5100	8.768748	0.263659	-268.129188	215.412702	-0.934968	9.939699	-0.002327710
$2s8d$	^{9}Be	6000	8.769246	0.263565	-268.126803	215.426995	-0.934971	9.936159	-0.002327011
		6900	8.769645	0.263536	-268.136303	215.437574	-0.934971	9.935061	-0.002327012
	$^{\infty}$Be	6900	8.771261	0.263579	-268.202480	215.477363	-0.908577	9.936711	-0.002326923
		4200	8.762599	0.263948	-268.001648	215.252739	-0.935364	9.950613	-0.002328877
		5100	8.764758	0.263884	-268.060442	215.308225	-0.935384	9.948204	-0.002329182
$2s9d$	^{9}Be	6000	8.766114	0.263813	-268.081960	215.343651	-0.935394	9.945525	-0.002328585
		6900	8.766759	0.263796	-268.092858	215.360177	-0.935396	9.944869	-0.002328320
	$^{\infty}$Be	6900	8.768376	0.263840	-268.159058	215.399986	-0.908997	9.946519	-0.002328232
		4200	0.264321	8.758158	-267.905564	215.134202	-0.935602	9.964658	-0.002329337
		5100	0.264157	8.759324	-267.930308	215.166584	-0.935605	9.958500	-0.002329258
$2s10d$	^{9}Be	6000	0.263989	8.761740	-267.963175	215.230472	-0.935620	9.952138	-0.002327946
		6900	0.263933	8.762366	-267.975800	215.247253	-0.935624	9.950058	-0.002327836
	$^{\infty}$Be	6900	0.263977	8.763983	-268.041978	215.287050	-0.909219	9.951710	-0.002327747

nine ^{1}D states of ^{9}Be and $^\infty$Be. $1s^2$, which is common to all configurations, is omitted from the configuration designation of the state (e.g. configuration $1s^2 2p^2$ is abbreviated as $2p^2$). The nonrelativistic energies are calculated with 14400 ECGs and the relativistic corrections are calculated with 6900 ECGs. All values given in a.u.

State	E_r (^{9}Be)	E_r ($^\infty$Be)
$2p^2$	-14.409615494	-14.410501338
$2s3d$	-14.375234551	-14.376134107
$2s4d$	-14.355403651	-14.356304503
$2s5d$	-14.345281845	-14.346182454
$2s6d$	-14.339591696	-14.340492051
$2s7d$	-14.336101396	-14.337001568
$2s8d$	-14.333812562	-14.334712607
$2s9d$	-14.332232910	-14.333132865
$2s10d$	-14.331094659	-14.331994546

owest nine ^{1}D states of the beryllium atom. $1s^2$, which is common to all configurations, is omitted from the configuration designation of the state (e.g. configuration $1s^22p^2$ is abbreviated as $2p^2$). The transition energies are calculated for $^\infty$Be and ^{9}Be without the relativistic corrections (ΔE_{nr}) using the total nonrelativistic energies obtained with 14400 ECGs, and with the addition of the relativistic correction ΔE_r calculated with 6900 ECGs. The estimates of the uncertainties of the transition energies calculated at the ΔE_{nr} (^{9}Be) + ΔE_r (^{9}Be) level are shown in parenthesis. The estimates correspond to the uncertainties due to using incomplete basis sets in the calculations of the nonrelativistic energies and the relativistic corrections (not to neglecting higher order effects). All energies are given in cm^{-1}.

Transition	ΔE_{nr} ($^\infty$Be)	ΔE_{nr} (^{9}Be)	ΔE_{nr} (^{9}Be) + ΔE_r ($^\infty$Be)	ΔE_{nr} (^{9}Be) + ΔE_r (^{9}Be)	Experiment
$2p^2 \rightarrow 2s3d$	7552.710	7555.727	7545.752	7545.745(0.020)	7545.8558(0.0215)
$2s3d \rightarrow 2s4d$	4354.747	4355.029	4352.378	4352.379(0.020)	4352.5568(0.0705)
$2s4d \rightarrow 2s5d$	2222.133	2222.080	2221.479	2221.480(0.030)	2221.446(0.10)
$2s5d \rightarrow 2s6d$	1249.149	1249.093	1248.843	1248.843(0.030)	1248.814(0.13)
$2s6d \rightarrow 2s7d$	766.252	766.212	766.032	766.032(0.080)	766.33(0.17)
$2s7d \rightarrow 2s8d$	502.511	502.483	502.341	502.341(0.080)	502.37(0.16)
$2s8d \rightarrow 2s9d$	347.001	346.981	346.694	346.694(0.090)	347.03(0.19)
$2s9d \rightarrow 2s10d$	249.726	249.711	249.817	249.817(0.090)	249.03(0.30)